Journal of the Society for Cardiovascular Angiography & Interventions 5 (2026) 105674

JSCAI

The official journal of the Society for Cardiovascular Angiography & Interventions

Original Research

Impact of Suspected Intraluminal Thrombus on Angiographic Outcomes in Patients Treated With Drug-Coated Balloon Angioplasty

Kotaro Miyashita, MD [a,b,c,†], Chun-Ting Shih, MD [a,b,d,†], Emiliano Bianchini, MD [a,†], Asahi Oshima, MD [a,b], Nozomu Kanehama, MD [a,b], Tsung-Ying Tsai, MD, PhD [a,b], Maya Miyashita, BSc [b], Antonio Colombo, MD [e], Bernhard Reimers, MD [e], Sandeep Basavarajaiah, MD, PhD [f], Faisal Sharif, MD, PhD [a], Luca Testa, MD, PhD [g], Carlo Di Mario, MD, PhD [h], Roberto Nerla, MD [i], Bernardo Cortese, MD, PhD [j], Scot Garg, MD, PhD [k,l], Jouke Dijkstra, PhD [m], Yoshinobu Onuma, MD, PhD [a,b], Patrick W. Serruys, MD, PhD [a,b,*]

[a] *School of Medicine, University of Galway, Galway, Ireland;* [b] *CORRIB Research Centre for Advanced Imaging and Core Lab, University of Galway, Galway, Ireland;* [c] *Department of Cardiology, Ageo Central General Hospital, Ageo, Japan;* [d] *Division of Cardiology, Department of Internal Medicine, Kaohsiung Chang Gung Memorial Hospital, Kaohsiung, Taiwan;* [e] *Humanitas Clinical and Research Center, IRCCS, Rozzano, Milan, Italy;* [f] *Heartlands Hospital, University Hospitals, Birmingham, United Kingdom;* [g] *Department of Cardiology, IRCCS Policlinico San Donato, San Donato Milanese, Milan, Italy;* [h] *Structural Interventional Cardiology, Department of Experimental and Clinical Medicine, Careggi University Hospital, Florence, Italy;* [i] *Department of Cardio-Thoracic GVM Care and Research, Maria Cecilia Hospital, Cotignola, Italy;* [j] *Cardiovascular Research Center, Fondazione Ricerca e Innovazione Cardiovascolare, Milan, Italy;* [k] *Department of Cardiology, Royal Blackburn Hospital, Blackburn, United Kingdom;* [l] *School of Medicine, University of Central Lancashire, Preston, United Kingdom;* [m] *Division of Image Processing, Department of Radiology, Leiden University Medical Center, Leiden, the Netherlands*

ABSTRACT

Background: The impact of suspected intraluminal thrombus (SIT) on angiographic outcomes in patients with small-vessel coronary artery disease treated with drug-coated balloons (DCB) remains unclear.

Methods: In the TReAtmeNt of Small Coronary Vessels: MagicTouch Sirolimus Coated Balloon (TRANSFORM I) substudy, optical coherence tomography was performed after predilation and before DCB use in 104 lesions (97 patients) to confirm the presence or absence of SIT. SIT was located in the dissected area, attached to the luminal surface (LS), or to the tip of the dissection flap. Artificial intelligence–driven analyses quantified the SIT volume and its optical characteristics (intensity, attenuation, and backscattering) to help differentiate red from white SIT. Quantitative coronary angiography and angiography-derived fractional flow reserve were assessed at the 6-month follow-up.

Results: Suspected intraluminal thrombus was identified in 46 of 104 lesions (44.2%). At 6 months, SIT lesions compared with non-SIT lesions had smaller minimum lumen diameters (1.21 vs 1.32 mm, $P = .03$), larger percent diameter stenoses (42% vs 36%, $P = .03$), and higher rates of binary restenosis (37.0% vs 13.8%, $P = .01$). Subgroup analyses did not demonstrate any significant interaction between the DCB type and the impact of SIT on worse angiographic outcomes ($P_{interaction} = .391$). In multivariable logistic regression, LS SIT (odds ratio, 3.66; 95% CI, 1.11-12.83; $P = .036$) and the DCB type (MagicTouch vs SeQuent, odds ratio, 4.11; 95% CI, 1.14-13.88; $P = .015$) emerged as independent predictors of binary restenosis.

Conclusions: Despite comparable postprocedural anatomic and physiological results, the observation of LS SIT on optical coherence tomography after predilatation and before DCB angioplasty was associated with adverse angiographic outcomes at 6 months.

Abbreviations: %DS, percent diameter stenosis; DCB, drug-coated balloon; MLD, minimum lumen diameter; OCT, optical coherence tomography; PCI, percutaneous coronary intervention; QCA, quantitative coronary angiography; SIT, suspected intraluminal thrombus.

Keywords: binary restenosis; coronary dissection; drug-coated balloon; intraluminal thrombus; Murray law-based quantitative flow ratio; optical coherence tomography.

* Corresponding author: patrick.serruys@nuigalway.ie (P.W. Serruys).

† Co-first authors.

https://doi.org/10.1016/j.jscai.2026.105674

Received 2 April 2026; Received in revised form 19 August 2026; Accepted 21 August 2026; Available online 15 October 2026

2772-9303/© 2026 The Author(s). Published by Elsevier Inc. on behalf of the Society for Cardiovascular Angiography & Interventions Foundation. This is an open access article under the CC BY license (http://creativecommons.org/licenses/by/4.0/).

Introduction

Over the past decade, drug-coated balloons (DCB) have emerged as a valuable alternative to drug-eluting stents in the percutaneous treatment of coronary artery disease.[1,2] In line with the "leave nothing behind" approach, DCB have shown comparable outcomes to drug-eluting stents in terms of target lesion failure, particularly in the treatment of "small" vessel coronary artery disease.[3–6]

Using intravascular imaging to guide DCB procedures helps ensure optimal balloon-to-vessel sizing and improves the selection of treatment strategies.[3,7,8] In addition, intravascular imaging, particularly optical coherence tomography (OCT), offers detailed insights into various microscopic findings, many of which are still being studied to understand their effects on outcomes following DCB-only angioplasty. Notably, although the presence and extent of intimal dissections have been identified as predictors of late lumen enlargement,[8–11] the impact of other findings, such as the presence of suspected intraluminal thrombus (SIT),[12,13] has yet to be investigated as a potential contributor to poorer functional and/or angiographic outcomes during follow-up.

Several preclinical studies in animal models have highlighted the role of platelets in vascular healing following injury, a process linked to the release of platelet-derived growth factor (PDGF) from activated platelets adhering to exposed collagen components of the arterial media.[11,14–17] The presence and extent of different types of SIT, and whether they influence coronary artery healing by potentially modulating the biological effects of the antiproliferative drug released by the DCB, have also not yet been investigated.

Therefore, the current study aimed to characterize the presence, morphometric parameters, and angiographic impact of SIT, as identified by OCT performed immediately pre-DCB angioplasty, using data from the TReAtmeNt of Small Coronary Vessels: MagicTouch Sirolimus Coated Balloon (TRANSFORM I) cohort, in which patients were randomized to receive 1 of 2 different DCB.

Methods

Study design, population, and methods of analysis

The TRANSFORM I study (NCT03913832) was a prospective, randomized, multicenter, open-label noninferiority trial conducted across several European centers.[18] A total of 121 patients presenting with either stabilized acute coronary syndrome or chronic coronary syndrome and having at least 1 de novo coronary lesion in a "small" vessel, defined by a reference vessel diameter <2.75 mm on quantitative coronary angiography (QCA), were enrolled.

Key inclusion and exclusion criteria are detailed in the previous publication.[17] Following successful predilatation, defined as the absence of: (1) major angiographic dissections (National Heart, Lung, and Blood Institute types C, D, E, or F); and (2) a thrombolysis in myocardial infarction flow grade ≤2, eligible patients were randomized in a 1:1 fashion to receive either the MagicTouch sirolimus-coated balloon (SCB) or the SeQuent Please Neo paclitaxel-coated balloon (PCB). The protocol adhered to the Declaration of Helsinki and received approval from all local institutional ethics committees. All participants provided informed consent prior to enrollment. As part of the procedural protocol, OCT was systematically performed after successful predilatation and before DCB treatment, allowing for lumen-based balloon sizing and retrospective assessment of dissection characteristics. Angiographic follow-up was conducted at 6 months to evaluate treatment outcomes. The TRANSFORM I study randomized 121 patients (129 lesions); however, after excluding patients who withdrew consent (n = 3) or lesions with bailout stenting (n = 4), unanalyzable QCA at baseline (n = 3), refusal of follow-up (n = 2), and poor OCT image quality (n = 13) because of insufficient blood clearance, a total of 97 patients (104 lesions) with OCT and 6-month angiographic follow-up remained for this subanalysis (Figure 1). The present analysis was not prespecified in the original TRANSFORM I protocol and should, therefore, be considered a retrospective post hoc exploratory analysis.

Study objectives (all post hoc analyses)

- To detect and characterize SIT immediately after lesion preparation and before DCB angioplasty through analysis of their frequency, location, and quantitative morphometric, volumetric, and optical characteristics.
- To investigate the link between the various types and locations of SIT and 6-month angiographic outcomes, following percutaneous coronary intervention (PCI) using PCB or SCB.

The end point parameters of this study were 6-month lesion-level angiographic measures consisting of QCA-derived minimum lumen diameter (MLD), percent diameter stenosis (%DS), binary restenosis, net lumen gain (mm), late lumen loss (mm), and μFR value, in lesions with or without SIT.

Thrombus detection, delineation, intraluminal localization, and optical characterization by OCT analysis

Optical coherence tomography imaging was performed using the OPTIS Integrated System with the Dragonfly imaging catheter (Abbott Vascular). OCT imaging analyses were conducted retrospectively offline by an independent core laboratory using dedicated software (QCU-CMS [Leiden University Medical Center]), using the original pullback images acquired at 0.1 mm/frame or 0.2 mm/frame.[19] The OCT image after predilatation (pre-DCB dilatation) was used to detect and evaluate SIT. First, lumen contours, including any dissections, were automatically delineated by the software and manually adjusted as needed to ensure accurate vessel boundary definition.

Next, all SIT were identified and traced on each cross-section, with their presence and extent independently adjudicated by 3 experienced analysts certified in OCT interpretation. Thrombus was defined as an irregular mass protruding into the lumen, with a clear attenuation boundary separating it from the point of attachment to the lumen (Figure 1). SIT were reviewed independently, and any disagreements were resolved by consensus. SIT were classified based on their location and attachment into 3 types (Figure 2): (1) SIT attached to the luminal surface (LS)—SIT contiguous with the intima but not involved in a dissection area; (2) SIT attached to the tip of the dissection flap (DF)—SIT adherent to or extending from the tip of a visible DF; and (3) SIT sitting in the dissection cavity and adherent to the dissected lumen (cul-de-sac).

Differentiation in red or white thrombus

In addition, analysts further classified each SIT into red or white thrombus. Red thrombus was defined as a high-backscattering mass with signal attenuation and shadowing behind it. In contrast, white thrombus was defined as a signal-rich, low-backscattering mass without attenuation or shadowing behind it. The software also automatically provided quantitative measurements of the attenuation coefficient, backscattering, and grayscale intensity within each traced region of interest (Figure 3 and Supplemental Video 1).[19] The maximum, median, mean, SD, as well as the 5th, 10th, 90th, and 95th percentiles of the signal distribution were calculated for each region of interest.

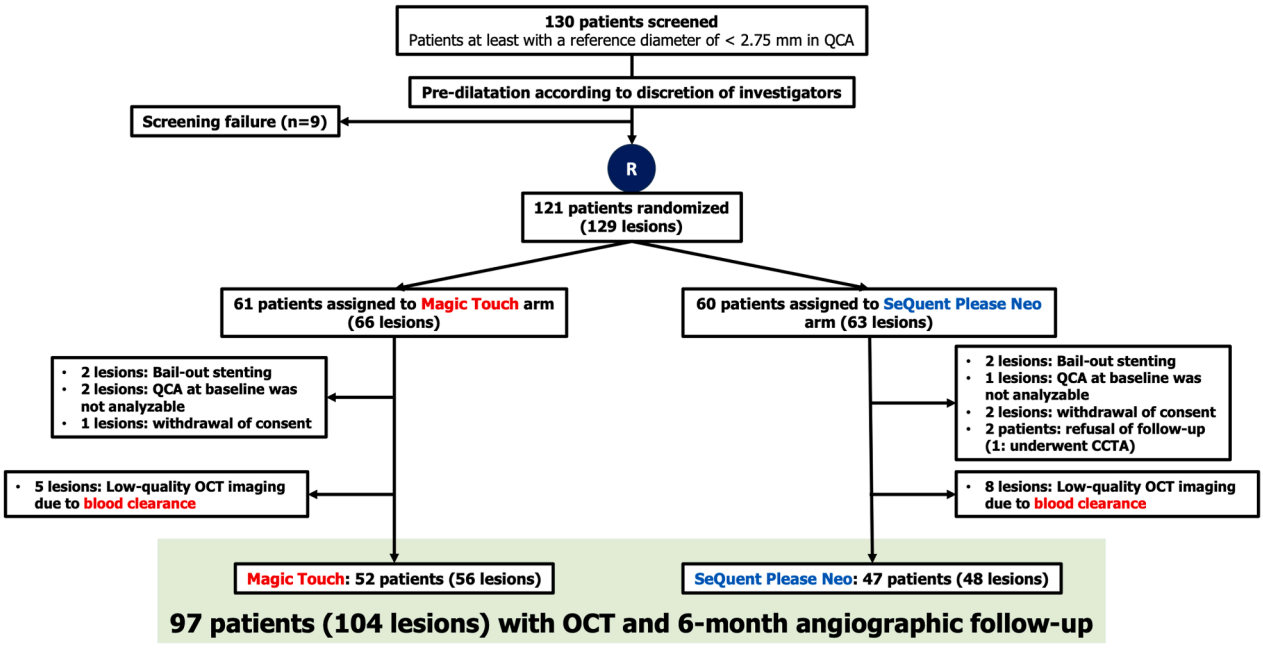

Figure 1.
Study flowchart. A total of 97 patients (104 lesions) underwent optical coherence tomography (OCT) imaging before drug-coated balloon angioplasty and completed 6-month angiographic follow-up (MagicTouch, n = 52 patients; SeQuent Please Neo, n = 47 patients). CCTA, coronary computed tomography angiography; QCA, quantitative coronary angiography.

To assess interobserver reproducibility for the following: (1) lumen area and (2) thrombus volume, 2 analysts independently evaluated the same OCT cross-sections from 10 randomly selected patients. After independently contouring the SIT regions of interest, their resulting continuous morphometric parameters (lumen area and thrombus volume) were assessed and compared by calculating the intraclass correlation coefficient (2-way random effects, absolute agreement). In addition, linear regression analysis with the regression equation and the coefficient of determination (R^2) was performed (Supplemental Figure S1).

QCA and quantitative flow ratio analyses

Quantitative coronary angiography and Murray law–based quantitative flow ratio (μFR) were performed by an independent academic core laboratory (CORRIB lab, University of Galway, Ireland) using the CAAS Workstation (Pie Medical Imaging) for QCA and the AngioPlus system (Pulse Medical Imaging Technology) for μFR computation. QCA and μFR were systematically performed at 3 time points in all available cases: baseline (pre-PCI), immediately after DCB angioplasty, and at the 6-month follow-up angiography. μFR is a computational method applied to a single angiographic view that considers side branch diameters in the computation of fractal flow division,[20] and has recently been shown to have similar diagnostic accuracy to 3-dimensional quantitative flow ratio, and a correlation of r = 0.90 ($P < .001$) and acceptable agreement with wire-based fractional flow reserve.[21,22] Angiographic-derived index of microcirculatory resistance (μFR-derived) was also collected.

Statistical analysis

Analyses were conducted at the vessel-level, with subjects divided into 2 groups: vessels with SIT before DCB, and vessels without SIT before DCB. Continuous variables were tested for normal distribution using the Shapiro-Wilk test and Q-Q plot visual examination, and were compared using an unpaired *t* test or the Mann-Whitney U nonparametric test, when appropriate. Data were expressed as means (SD) or median and interquartile range. Categorical variables were compared using χ^2 or Fisher exact test as appropriate and expressed as frequencies and percentages.

The associations between SIT at different luminal locations and the rates of follow-up binary restenosis were tested using univariate and multivariable logistic regression analyses. Multivariable models included the DCB type (PCB vs SCB) and dissection volume, as these could represent potential confounders. All 3 SIT locations were included in the multivariable model. Multicollinearity was assessed using the variance inflation factor, with variables having a variance inflation factor >10 removed from the multivariable model.

Results

Among the 104 lesions (97 patients) with evaluable OCT and angiographic follow-up, 46 lesions (44.2%) in 44 patients had detectable SIT, whereas 58 lesions (55.8%) in 53 patients had no SIT (Figure 1). Thrombi were located attached to the LS in 30 lesions (65.2%), the tip of the DF in 37 lesions (80.4%), and sitting in the cul-de-sac cavity in 21 lesions (45.7%).

Baseline and procedural characteristics

Baseline clinical characteristics were similar between patients with or without SIT (Table 1).

Procedural characteristics are shown in Table 2. The distribution of target vessels and reference vessel diameters was comparable between groups. Lesions with SIT had a smaller pre-PCI MLD (0.83 [0.30] mm vs 0.98 [0.29] mm, $P < .01$) and a larger pre-PCI %DS (60% [52-67] vs 52% [45-64], $P = .01$) compared with non-SIT lesions. The maximum predilation balloon length was longer in SIT lesions (19.6 [6.1] mm vs 16.8 [4.5] mm, $P = .01$). Other balloon and DCB characteristics, as well as the incidence of post-PCI angiographic dissection, were similar between groups.

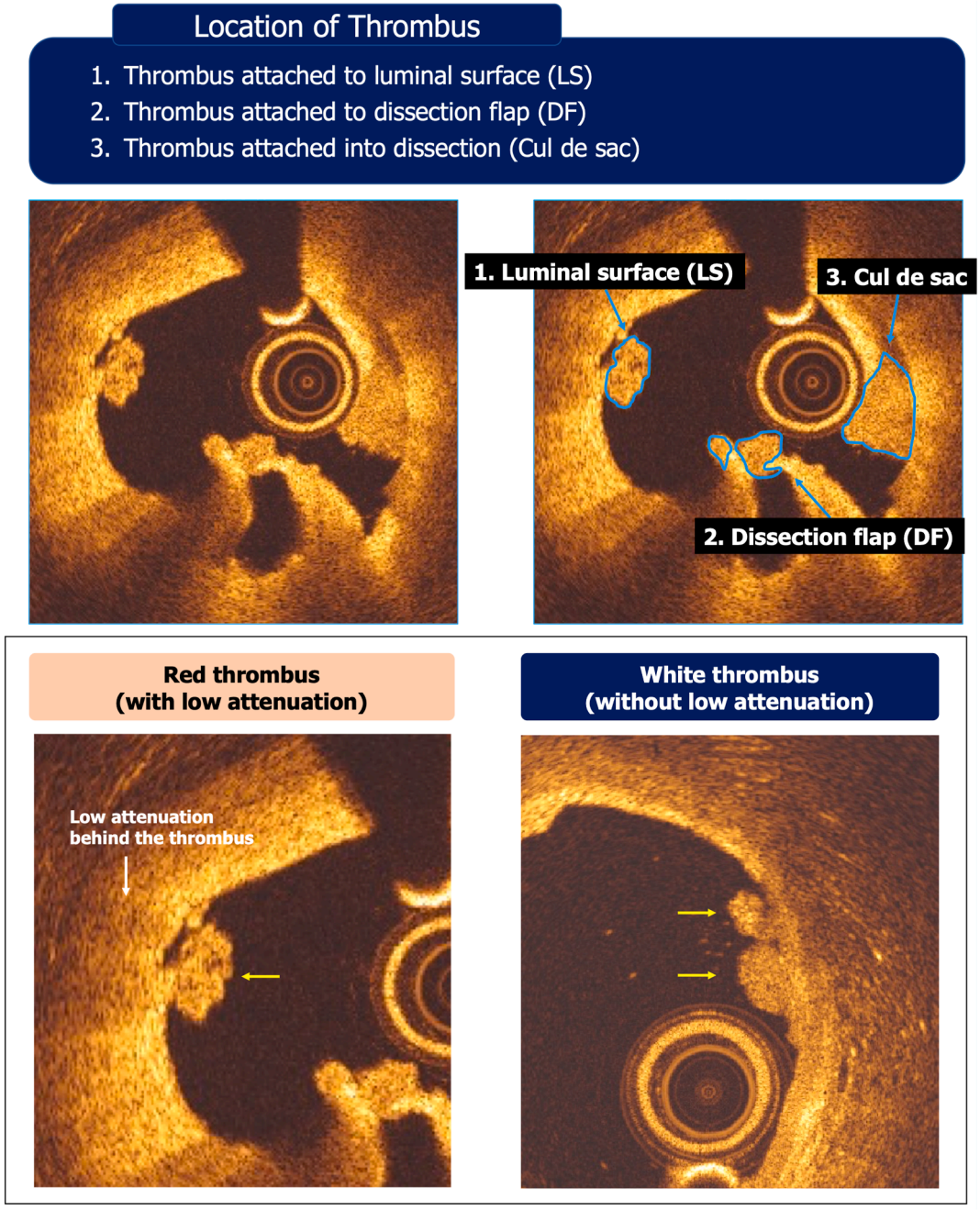

Figure 2.
Classifications of intraluminal thrombus by location and optical characteristics. Representative optical coherence tomography (OCT) cross-sectional images illustrating intraluminal thrombus classified according to both location and optical properties. By location and attachment: (1) luminal surface (LS)—thrombus contiguous with the intima not involving a dissection area; (2) dissection flap (DF)—thrombus adherent to or extending from the tip of a visible dissection flap; and (3) cul-de-sac—thrombus sitting in the dissection cavity and adherent to the dissected lumen. Blue area indicates the traced thrombus contours.

OCT-derived and angiographic results

Optical coherence tomography–derived parameters at baseline, and QCA data and angiography-derived physiological parameters at baseline and 6-month angiographic follow-up are summarized in Table 3.

Baseline μFR was significantly lower in SIT compared with non-SIT lesions (0.76 [0.62-0.88] vs 0.85 [0.73-0.91], $P = .03$). Angiography- and OCT-derived markers of successful DCB angioplasty were similar between lesions with and without SIT, except for the proportion of lesions with a μFR >0.80 after DCB angioplasty, which was higher in the SIT group (93.5% [44/58] vs 75.9% [43/46], $P = .02$). At 6 months, lesions in the SIT group had a smaller MLD (1.21 [0.93-1.44] mm vs 1.32 [1.15-1.52] mm, $P = .03$), a larger %DS (42% [32-52] vs 36% [28-45], $P = .03$), more frequent binary restenosis (36.9% vs 13.8%, $P = .01$, Figure 4), lower μFR (0.85 [0.78-0.93] vs 0.90 [0.87-0.95], $P = .01$), and higher rates of lesions with a μFR ≤0.80 (30.4% vs 12.1%, $P = .04$). The baseline and 6-month follow-up angiographic differences between lesions with SIT or non-SIT according to different DCB types are presented in Supplemental Table S1 and Supplemental Figure S2.

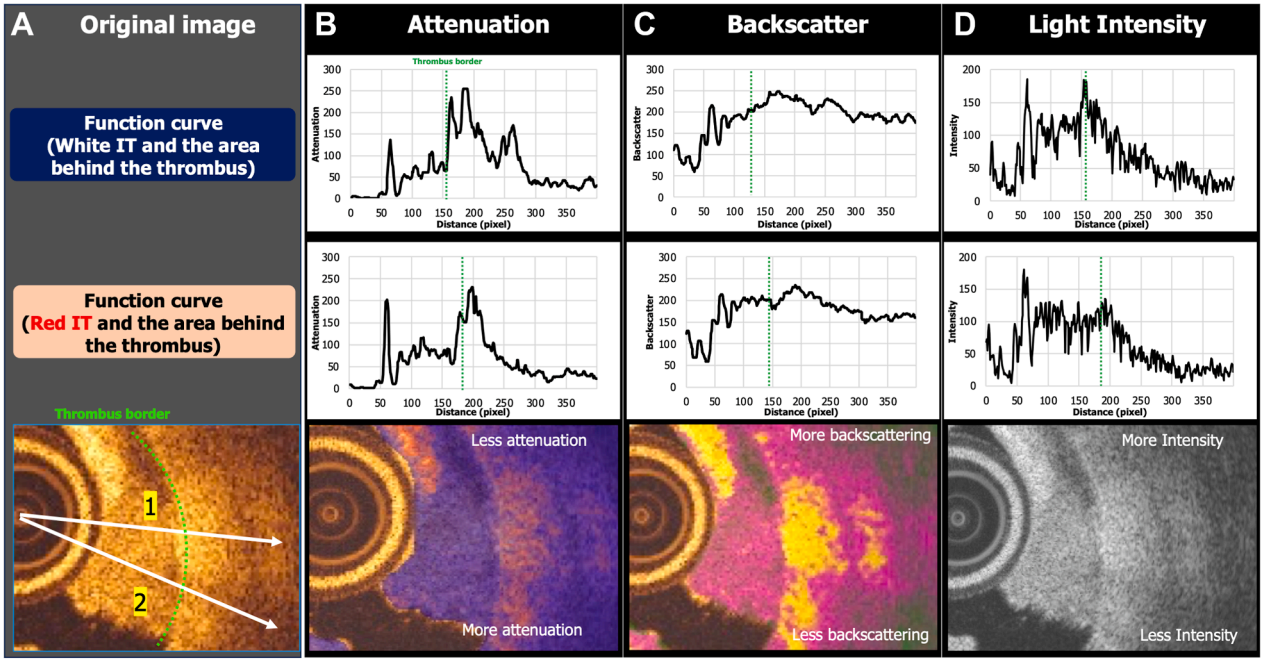

Figure 3.
Optical coherence tomography image example of light attenuation, backscatter, and light intensity analyses of thrombus and the wall area behind the thrombus. An image example of light property analysis is presented. Based on the original image (**A**), the dedicated software fully automatically computed 3 components of light property analysis: (**B**) light attenuation, (**C**) light backscatter, and (**D**) light intensity. The upper panels indicate the function curves of each parameter along lines 1 and 2. The lower panels show the color-coded images of each parameter. The dotted green line denotes the thrombus border. IT, intraluminal thrombus.

OCT-derived thrombus characteristics and physiological correlates

The quantitative morphometric analysis of SIT, both overall and by location, is summarized in Table 4.

Quantitative optical analysis across SIT types

Quantitative analyses showed significant differences in morphometric and optical parameters across the 3 SIT locations (Supplemental Table S2). The mean SIT area was larger in LS (0.046 mm^2) and cul-de-sac (0.042 mm^2) SIT compared with DF SIT (0.034 mm^2, ANOVA $P = .019$, Kruskal-Wallis $P < .001$). Similarly, the SIT perimeter was greater in LS (1.151 mm) and cul-de-sac (1.088 mm) SIT compared with DF SIT (0.924 mm, $P = .001$).

In attenuation analyses, there were no significant differences among the 3 SIT types.

In contrast, backscatter and intensity parameters showed consistent patterns. Maximum and mean backscatter were lowest in DF SIT (6.40 and 5.40) compared with LS (6.61 and 5.76) and cul-de-sac (6.67 and 5.83, all $P < .01$) SIT. Similarly, maximum, mean, and median intensity values were lower in DF SIT (725, 208, and 187, respectively) compared to LS (862, 240, and 216, respectively) and cul-de-sac (883, 242, and 219, respectively; all $P < .001$) SIT.

Attenuation analyses of SIT appeared to differentiate what was adjudicated by analysts as red or white thrombus (Supplemental Table S3 and Supplemental Figure S3). Maximum (2.52 vs 2.16, $P = .011$), mean (1.23 vs 1.02, $P = .009$), and median (1.20 vs 0.98, $P = .010$) attenuation values were all significantly greater for red compared to white thrombus. Backscatter parameters showed a similar trend, with red thrombus having higher maximum (6.77 vs 6.51, $P = .015$), mean (5.92 vs 5.60, $P = .013$), and median values (5.98 vs 5.63, $P = .006$). Maximum intensity analysis values were significantly higher with red thrombus (821 vs 733, $P = .022$).

Light property analyses of the area behind the SIT (Supplemental Table S4 and Supplemental Video 1) revealed higher mean and median attenuation values with white thrombus compared to red thrombus (0.99 vs 0.84, $P = .026$; 0.89 vs 0.74, $P = .026$). Conversely, mean and median backscatter (5.89 and 5.88 vs 6.11 and 6.10, both $P < .05$) and intensity (82 and 56 vs 114 and 77, both $P < .05$) were lower with red thrombus.

Multivariable model and further subgroup analyses

Univariate and multivariable logistic regression analyses were performed to test the association between SIT at various sites and binary restenosis (Table 5). In the univariate analysis, the presence of LS (odds

Table 1. Baseline patient characteristics

Characteristics	Overall (N = 97)	Non-SIT (n = 53)	SIT (n = 44)	*P* value
Age, y	66.8 ± 9.4	65.8 ± 9.4	68.1 ± 9.3	.23
Male sex	84 (86.6)	44 (83.0)	40 (90.9)	.37
Current smoker	19 (19.6)	12 (22.6)	7 (15.9)	.57
Medically treated diabetes	23 (23.7)	12 (22.6)	11 (25.0)	.97
Insulin	5 (5.2)	3 (5.7)	2 (4.5)	>.99
Hypertension	79 (81.4)	43 (81.1)	36 (81.8)	>.99
Dyslipidemia	80 (82.5)	45 (84.9)	35 (79.5)	.67
Previous MI	28 (28.9)	17 (32.1)	11 (25.0)	.59
Peripheral vascular disease	2 (2.1)	0 (0.0)	2 (4.5)	.20
COPD	5 (5.2)	3 (5.7)	2 (4.5)	>.99
History of heart failure	6 (6.2)	4 (7.5)	2 (4.5)	.69
History of major bleeding	1 (1.0)	0 (0.0)	1 (2.3)	.45
Renal failure	1 (1.0)	0 (0.0)	1 (2.3)	.45
Previous PCI	49 (50.5)	27 (50.9)	22 (50.0)	>.99
Previous CABG	2 (2.1)	2 (3.8)	0 (0.0)	.50
Previous stroke	5 (5.2)	2 (3.8)	3 (6.8)	.66
Acute coronary syndrome	5 (5.2)	3 (5.7)	2 (4.5)	>.99
Chronic coronar syndrome	92 (94.8)	50 (94.3)	42 (95.5)	>.99

Values are mean ± SD or n (%).
CABG, coronary artery bypass grafting; COPD, chronic obstructive pulmonary disease; SIT, suspected intraluminal thrombus; MI, myocardial infarction; PCI, percutaneous coronary intervention.

Table 2. Procedural characteristics

Characteristics	Total (N = 104)	Non-SIT (n = 58)	SIT (n = 46)	*P* value
Left anterior descending artery	29 (27.9)	16 (27.6)	13 (28.3)	>.99
Left circumflex artery	52 (50.0)	26 (44.8)	26 (56.5)	.32
Right coronary artery	23 (22.1)	16 (27.6)	7 (15.2)	.20
QCA reference vessel diameter, mm	2.06 ± 0.5	2.1 ± 0.4	2.1 ± 0.5	.76
QCA lesion length, mm	13.0 ± 7.8	12.3 ± 7.4	14.0 ± 8.4	.31
Vessels with bifurcation lesion	32 (30.8)	17 (29.3)	15 (32.6)	.88
Vessel with AHA type B2/C lesion	34.0 (32.7)	16.0 (27.6)	18.0 (39.1)	.30
Pre-PCI QCA minimum lumen diameter, mm	0.91 ± 0.30	0.98 ± 0.29	0.83 ± 0.3	<.01
Pre-PCI QCA diameter stenosis, %	55.0 (48.0-66.0)	52.0 (45.0-63.8)	60.0 (52.3-67.0)	.01
Max predilation balloon diameter, mm	2.5 (2.0-2.5)	2.5 (2.0-2.5)	2.5 (2.0-2.5)	.89
Max predilation balloon length, mm	18.0 ± 5.4	16.8 ± 4.5	19.6 ± 6.1	.01
Max predilation pressure, atm	14.0 (12.0-16.0)	14.0 (12.0-16.0)	14.0 (10.0-16.0)	.44
Noncompliant balloon	32 (30.8)	17 (29.3)	15 (32.6)	.88
Compliant balloon	72 (69.2)	41 (70.7)	31 (67.4)	.88
DCB diameter, mm	2.5 (2.2-2.8)	2.5 (2.2-2.8)	2.5 (2.2-2.5)	.66
DCB length, mm	23.1 ± 6.0	22.4 ± 5.9	24.0 ± 6.0	.21
DCB inflation time, s	60.0 (60.0-87.5)	60.0 (60.0-90.0)	60.0 (60.0-80.0)	.65
DCB maximum pressure, atm	8.0 (8.0-10.0)	8.0 (8.0-10.0)	9.0 (8.0-10.2)	.15
Balloon/artery ratio	1.2 ± 0.3	1.2 ± 0.3	1.3 ± 0.3	.59
DCB type: MagicTouch SCB	56 (53.8)	33 (56.9)	23 (50.0)	.62
DCB type: SeQuent Please Neo PCB	48 (46.2)	25 (43.1)	23 (50.0)	.62
Post-PCI angiographic dissection	17.0 (16.3)	8.0 (13.8)	9.0 (19.6)	.56

Values are mean ± SD, median (IQR), or n (%).
AHA, American Heart Association; DCB, drug-coated balloon; PCB, paclitaxel-coated balloon; PCI, percutaneous coronary intervention; QCA, quantitative coronary angiography; SCB, sirolimus-coated balloon; SIT, suspected intraluminal thrombus.

Table 3. OCT derived, angiographic, and physiological parameters at baseline, after DCB angioplasty, and at 6 month follow-up

Variables	Total (N = 104)	Non-SIT (n = 58)	SIT (n = 46)	*P* value
Baseline angiographic parameters				
Pre-PCI QCA minimum lumen diameter, mm	0.91 ± 0.3	0.98 ± 0.29	0.83 ± 0.3	.01
Pre-PCI QCA diameter stenosis, %	55 (48-66)	52 (45-63.75)	60 (52.25-67)	.01
μFR	0.81 (0.69-0.89)	0.85 (0.73-0.91)	0.76 (0.62-0.88)	.03
μFR >0.80	56 (53.8)	36 (62.1)	20 (43.5)	.09
Flow velocity (μFR), cm/s	16.1 (13.2-19.2)	16.2 (12.48-18.9)	15.6 (14.2-19.6)	.64
IMR	2.07 ± 0.65	2.2 ± 0.57	1.9 ± 0.71	.02
IMR >2.5	23 (22.1)	15 (25.9)	8 (17.4)	.43
Baseline OCT parameters				
Distal reference diameter, mm	2.27 ± 0.37	2.26 ± 0.40	2.27 ± 0.33	.92
Proximal reference diameter, mm	2.54 ± 0.39	2.52 ± 0.39	2.57 ± 0.39	.48
DCB/artery ratio	1.09 (0.94-1.23)	1.1 (0.89-1.23)	1.09 (0.97-1.23)	.94
Lesion length, mm	20 (14-25)	17 (13.6-25)	20 (15-26.68)	.35
Minimal lumen area, mm^2	2 (1.65-2.36)	1.96 (1.66-2.36)	2.03 (1.59-2.53)	.94
Angiographic and physiological results after DCB				
Post-PCI QCA minimum lumen diameter, mm	1.45 ± 0.31	1.47 ± 0.32	1.43 ± 0.31	.56
Post-PCI QCA diameter stenosis, %	31.4 ± 12.41	31.0 ± 12.37	32.0 ± 12.58	.69
μFR	0.91 (0.83-0.94)	0.91 (0.82-0.95)	0.92 (0.84-0.94)	.50
μFR >0.80	87 (83.7)	44 (75.9)	43 (93.5)	.02
Flow velocity (μFR), cm/s	16.9 (13.75-20.9)	17.3 (13.98-21.05)	16.25 (13.5-20.05)	.52
IMR	2.24 (1.94-2.62)	2.2 (1.87-2.6)	2.32 (2.02-2.65)	.27
IMR >2.5	34 (32.7)	17 (29.3)	17 (37)	.54
OCT parameters after predilatation				
Dissection volume, mm^3	2.21 (0.69-3.92)	1.64 (0.65-2.96)	2.97 (0.75-4.82)	.05
Longitudinal dissection length, mm	6.2 (3-10.6)	5 (2.9-11.3)	7.1 (4.05-10.15)	.19
Recoil, %	0.06 ± 0.14	0.06 ± 0.13	0.05 ± 0.15	.64
Angiographic and physiological results after 6-mo follow-up				
Minimal lumen diameter, mm	1.29 (1.02-1.5)	1.32 (1.15-1.52)	1.21 (0.93-1.44)	.03
QCA diameter stenosis, %	38.5 (28.75-49)	36 (28-45)	42 (31.75-52)	.03
Binary restenosis ≥50%, %	25 (24)	8 (13.8)	17 (36.9)	.01
Net lumen gain, mm	0.32 (0.12-0.64)	0.32 (0.15-0.51)	0.36 (0.06-0.72)	.95
Late lumen loss, mm	0.13 (–0.13 to 0.41)	0.10 (–0.14 to 0.38)	0.20 (–0.12 to 0.58)	.23
μFR	0.90 (0.83-0.93)	0.90 (0.87-0.95)	0.85 (0.78-0.93)	.01
μFR >0.80	83 (79.8)	51 (87.9)	32 (69.6)	.04
Flow velocity (μFR), cm/s	14.6 (12.3-16.92)	14.50 (12.12-16.98)	14.75 (12.5-16.9)	.51
IMR	2.47 ± 0.59	2.54 ± 0.55	2.37 ± 0.63	.15
IMR >2.5	51 (49)	34 (58.6)	17 (37)	.05

Values are presented as mean ± SD, median (IQR), or n (%).
μFR, Murray law–based quantitative flow ratio; DCB, drug-coated balloon; IMR, index of microcirculatory resistance; OCT, optical coherence tomography; PCI, percutaneous coronary intervention; QCA, quantitative coronary angiography; SIT, suspected intraluminal thrombus.

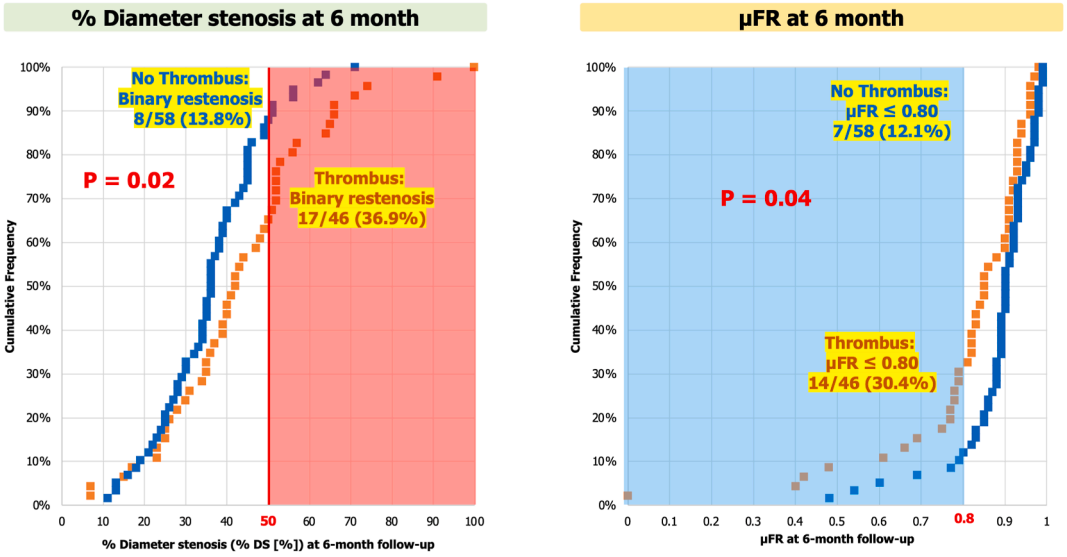

Figure 4.
Cumulative frequency plots of binary restenosis and μFR according to intraluminal thrombus. Orange dots show the thrombus group, and blue dots show the non-thrombus group. The red vertical line indicates the threshold for binary restenosis (% diameter stenosis ≥50%), and the blue vertical line shows the threshold for μFR (≤0.80). *P* value for the cumulative frequency curve was calculated using the Kolmogorov-Smirnov test. μFR, Murray law–based fractional flow reserve.

ratio [OR], 3.13; 95% CI, 1.21-8.14; $P = .018$) and cul-de-sac (OR, 3.14; 95% CI, 1.11-8.77; $P = .028$) SIT were significantly associated with binary restenosis, whereas DF SIT was not significant (OR, 2.48; 95% CI, 0.99-6.31; $P = .053$). In addition, the DCB type (SeQuent PCB vs MagicTouch SCB) was associated with a significantly higher risk of restenosis (OR, 3.59; 95% CI, 1.36-10.74; $P = .014$). In the multivariable analysis that included all 3 SIT locations, the DCB type, and dissection volume, only LS SIT (OR, 3.66; 95% CI, 1.11-12.83; $P = .036$) and the DCB type (OR, 4.11; 95% CI, 1.14-13.88; $P = .015$) remained independently associated with binary restenosis. Angiographic parameters at the 6-month follow-up for SIT or non-SIT lesions, according to the type of DCB, are shown in Supplemental Figure S3.

The association between SIT and 6-month follow-up binary restenosis was consistent across several subgroup analyses, including lesion complexity, pre-PCI μFR value, bifurcation lesion treatment, the type of DCB used, and the use of semicompliant or noncompliant balloons during lesion preparation (Supplemental Figure S3). The association between LS SIT and binary restenosis remained consistent in a sensitivity multivariable analysis adjusting for baseline lesion severity (pre-PCI MLD, pre-PCI %DS, baseline μFR, and the DCB type) (Supplemental Table S5). Similar findings were observed in a sensitivity analysis accounting for within-patient clustering using generalized estimating equations (Supplemental Table S6).

Table 4. Quantitative morphometric parameters of intraluminal thrombus

Parameter	Median (IQR)	Range
Total (N = 46)		
Total SIT area, mm^2	0.18 (0.06-0.72)	0.03-4.91
Total SIT, mm^3	0.02 (0.01-0.10)	0.00-0.49
Total mean diameter, mm	1.16 (0.54-2.86)	0.18-21.65
Total Perimeter, mm	5.94 (2.38-14.60)	0.72-106.75
Luminal surface (n = 30 [65.2%])		
Area, mm^2	0.08 (0.04-0.25)	0.02-3.97
Volume, mm^3	0.02 (0.01-0.05)	0.00-0.79
Mean diameter, mm	0.70 (0.25-1.65)	0.15-21.17
Perimeter, mm	3.63 (1.30-7.42)	0.72-104.80
Dissection tip (n = 37 [80.4%])		
Area, mm^2	0.08 (0.03-0.18)	0.00-1.80
Volume, mm^3	0.02 (0.01-0.04)	0.00-0.36
Mean diameter, mm	0.37 (0.11-1.04)	0.00-8.01
Perimeter, mm	2.59 (1.36-6.16)	0.26-36.89
Cul-de-sac (n = 21 [45.7%])		
Area, mm^2	0.06 (0.02-0.22)	0.01-3.81
Volume, mm^3	0.01 (0.00-0.04)	0.00-0.76
Mean diameter, mm	0.49 (0.17-1.14)	0.10-13.86
Perimeter, mm	2.65 (0.71-7.44)	0.43-75.16

SIT, suspected intraluminal thrombus.

Discussion

The main findings of the present study are as follows (Central Illustration):

1. Although postprocedural angiography-derived and OCT-derived markers of successful balloon angioplasty were mostly similar between lesions with and without SIT, at the 6-month follow-up, lesions with SIT exhibited smaller MLD, higher %DS, and consequently higher rates of binary restenosis compared to lesions without SIT.
2. The location of SIT was associated with the risk of binary restenosis during follow-up, with LS SIT having the strongest independent association with adverse angiographic outcomes.
3. The negative impact of SIT on follow-up angiographic outcomes was consistent across clinically relevant subgroups, including the DCB type (MagicTouch versus SeQuent). In multivariable models, both the presence of SIT and the type of DCB independently predicted binary restenosis, but no significant interaction was observed between the DCB type and the relationship of SIT with angiographic outcomes.

To our knowledge, this is the first study analyzing the impact of different morphometric features of SIT at various luminal locations on angiographic outcomes after DCB angioplasty. In the primary analysis of TRANSFORM I, Ninomiya et al[18] reported that a larger dissection volume after DCB angioplasty was associated with greater late lumen gain at 6 months. Although the dissection may promote drug uptake, retention, and lumen enlargement, our data suggest that SIT could attenuate this favorable effect, resulting in a smaller lumen size and higher restenosis during follow-up.

Table 5. Association of intraluminal thrombus with follow-up binary restenosis (logistic regression model)

Predictor	Univariate			Multivariable		
	Odds ratio	95% CI	*P* value	Odds ratio	95% CI	*P* value
IT at luminal surface	3.13	1.21-8.14	.018	3.66	1.11-12.83	.036
IT at cul-de-sac	3.14	1.11-8.77	.028	2.01	0.52-8.02	.311
IT at dissection tip	2.48	0.99-6.31	.053	1.36	0.35-4.85	.644
Dissection volume	0.97	0.83-1.10	.651	0.908	0.77-1.08	.279
DCB type	3.59	1.36-10.74	.014	4.11	1.41-13.88	.015

DCB, drug-coated balloon; IT, intraluminal thrombus.

In a recent observational study by Yamamoto et al,[10] residual thrombus burden after DCB treatment was independently associated with target lesion failure in patients with acute coronary syndrome. The rates of target lesion failure were similar between patients with a ruptured plaque and a small amount of residual thrombus and those with plaque erosion and a large amount of residual thrombus.[10]

The varying locations of SIT observed in this cohort may reflect different underlying mechanisms triggered during balloon angioplasty. SIT formation in cul-de-sac regions is primarily driven by blood stasis and extensive exposure of plaque components, which trigger activation of the coagulation cascade, leading to the development of a clot rich in fibrin and erythrocytes.[23,24] LS SIT following balloon angioplasty is less influenced by blood stasis and more by intimal tears or endothelial denudation caused by balloon inflation. These disruptions may trigger platelet adhesion and activation through exposure to von Willebrand factor, collagen, and other matrix components. The erosion exposes proteoglycan-rich structures, including hyaluronic acid, which further facilitates platelet adhesion and thrombus formation,[25] making LS SIT more likely to be platelet-rich.[26] In contrast, SIT at the DF tip may consist of a mixture of platelet-rich thrombus and disrupted material from the flap itself, which, in this location, is often difficult to distinguish from thrombus.[27] This partly explains the significant differences in attenuation, intensity, and backscattering observed among the 3 SIT types, especially in cases where SIT is attached to the DF tip.

Most thrombi were classified as white thrombus (n = 571 areas), while red thrombus was less common (n = 109 areas). Quantitative optical analysis confirmed significant differences in attenuation, backscatter, and intensity parameters between the 2 types of thrombus. The reliability of our visual classification is supported by Kaivosoja et al,[19] who demonstrated that OCT signal characteristics can effectively differentiate thrombus composition.[21]

Optical characteristics of the vessel wall located behind the red and white thrombus

The area behind the thrombus showed distinct light transmission properties depending on the type of thrombus. White thrombus was

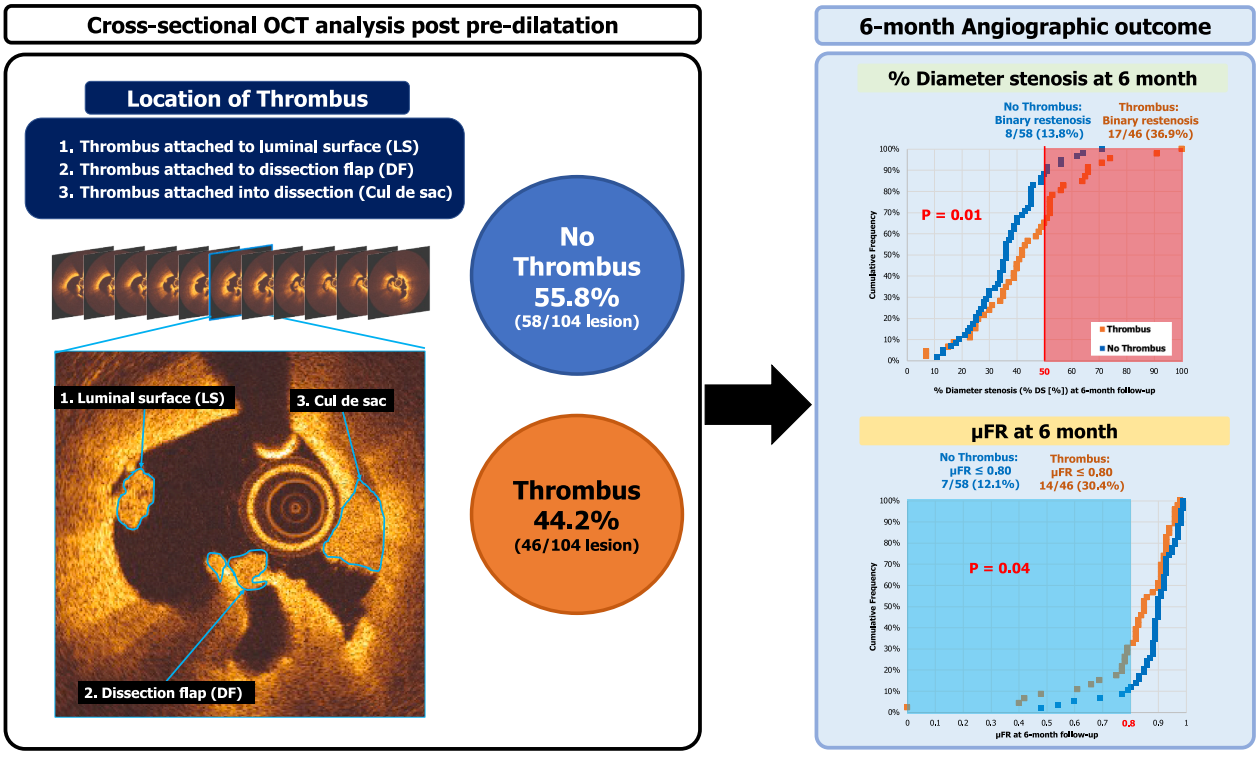

Central Illustration.

Impact of intraluminal thrombus detected by optical coherence tomography (OCT) after predilatation on 6-month angiographic and physiological outcomes. Cross-sectional OCT analysis immediately after predilatation identified intraluminal thrombus in 44.2% (46/104) attached to the luminal surface (LS), dissection flap (DF), or within the cul-de-sac. Lesions with thrombus demonstrated significantly greater angiographic diameter stenosis at 6 months (36.9% vs 13.8%, $P = .01$) and a higher prevalence of impaired physiological recovery (μFR ≤0.80: 30.4% vs 12.1%, $P = .04$) compared with lesions without thrombus. μFR, Murray law–based fractional flow reserve.

associated with lower attenuation and higher intensity, suggesting more efficient light transmission and less optical shadowing. Conversely, red thrombus produced a prominent shadowing effect, reflecting greater light absorption and scattering because of its fibrin network and erythrocyte count.

Intrinsic optical characteristics of red and white thrombus

Red thrombus had higher attenuation and backscatter than white thrombus, which aligns with its denser fibrin and erythrocyte content, resulting in more light scattering and signal loss.[28] In contrast, white thrombus, which is predominantly platelet-rich, exhibited low optical density and minimal shadowing with less attenuation. These optical characteristics are consistent with histopathologic findings from prior OCT validation studies.

Optical characteristics of thrombi related to their intraluminal location

Of note, LS SIT demonstrated backscatter values similar to those observed in visually adjudicated white thrombus areas. In contrast, SIT at the cul-de-sac exhibited significantly higher levels of backscatter, more akin to that of red thrombus. These data support the hypothesis that distinct mechanisms of thrombus formation operate during the procedure, contributing to the differences in thrombus composition. Importantly, although SIT at the DF tip was not significantly associated with binary restenosis at follow-up, SIT at the cul-de-sac and LS had a significant association, with the latter demonstrating the strongest correlation, which remained significant after multivariable adjustment.

Three main mechanisms may explain the negative association between SIT and DCB outcomes. First, SIT may physically hinder drug uptake by interposing between the balloon and the vessel wall or by filling the dissection cavity. Second, SIT itself may exert biological stimuli that promote neointimal formation and decrease drug efficacy. Activated platelets release PDGF, which has been shown in rodent and primate models to mediate smooth muscle cell migration and intimal thickening through the β-PDGF receptor pathway.[14,15] Third, SIT may be a marker of underlying plaque phenotype. Although our study cannot establish a direct relationship, previous investigations have reported that thin cap fibroatheromas and layered plaques are associated with more favorable angiographic outcomes after DCB angioplasty than fibrous or calcified plaques.[9,11]

This current study was not designed to assess plaque phenotype directly, and OCT-based classification of thin cap fibroatheromas or layered structures was not systematically performed. Nevertheless, it is conceivable that the adverse prognostic impact of SIT observed in our cohort may partially reflect interactions with these vulnerable plaque substrates. Platelet activation and thrombus formation are known to occur preferentially at sites of plaque rupture or erosion, which may counterbalance the expected benefit of enhanced drug uptake in such lesions.[9] Although our findings cannot establish a causal relationship, they highlight the importance of considering plaque morphology alongside thrombus in future imaging-based studies of DCB angioplasty.

Limitation

The results of the present study must be considered in light of the following limitations. First, this was a retrospective substudy with a limited sample size, which reduces statistical power and may introduce residual confounding factors. Second, although all patients were on DAPT post-DCB, the documentation of the specific P2Y12 inhibitors used and the duration of pretreatment was not systematically collected and should be, in the near future, the focus of investigation. Third, although residual thrombus burden after DCB angioplasty has been reported to predict target lesion failure, post-DCB OCT imaging was not available in the present study. Therefore, residual thrombus persistence after balloon inflation could not be assessed, and its potential relationship with the observed angiographic outcomes remains unknown. Fourth, the primary end point of this study was a 6-month angiographic surrogate end point, and the relationship between binary angiographic restenosis and subsequent long-term clinical outcomes remains uncertain. Fifth, histologic validation was not performed, and the identification of thrombus relied solely on optical characteristics. Finally, the limited sample size resulted in imprecise estimates in the multivariable sensitivity analysis, as reflected by the wide CI, and limited the statistical power for interaction analyses. Therefore, these exploratory findings should be interpreted with caution, and the absence of a statistically significant interaction between DCB type and SIT should not be interpreted as evidence of a consistent effect across DCB types.

Conclusion

Despite comparable postprocedural anatomic and physiological results, the observation of LS SIT on OCT after lesion predilatation and before DCB angioplasty was associated with smaller lumen dimensions and higher restenosis rates at the 6-month follow-up. These findings suggest that LS SIT may represent an exploratory OCT-derived marker of adverse angiographic outcomes after DCB angioplasty.

CRediT authorship contribution statement

Kotaro Miyashita: Writing – review & editing, Writing – original draft, Methodology, Formal analysis. **Chun-Ting Shih:** Visualization, Resources, Methodology, Investigation, Data curation. **Emiliano Bianchini:** Writing – review & editing, Writing – original draft, Methodology. **Asahi Oshima:** Resources, Data curation. **Nozomu Kanehama:** Investigation, Data curation. **Tsung-Ying Tsai:** Resources, Data curation. **Maya Miyashita:** Resources, Data curation. **Antonio Colombo:** Supervision. **Bernhard Reimers:** Supervision. **Sandeep Basavarajaiah:** Supervision. **Faisal Sharif:** Supervision. **Luca Testa:** Supervision. **Carlo Di Mario:** Supervision. **Roberto Nerla:** Supervision. **Bernardo Cortese:** Resources. **Scot Garg:** Writing – review & editing, Writing – original draft. **Jouke Dijkstra:** Validation, Supervision, Software, Formal analysis. **Yoshinobu Onuma:** Supervision. **Patrick W. Serruys:** Validation, Supervision, Conceptualization.

Acknowledgments

The authors thank all investigators of the TRANSFORM I study for their valuable contributions.

Declaration of competing interest

Kotaro Miyashita reports a research grant from OrbusNeich Medical K.K., outside the submitted work. Emiliano Bianchini received speaker's fees from Medtronic. Scot Garg reports consulting fees from BIOSENSORS. Patrick W. Serruys reports consulting fees from SMT,

Meril Life, Novartis, and Philips. The other authors declare no conflicts of interest.

Funding sources

This work was not supported by funding agencies in the public, commercial, or not-for-profit sectors.

Ethics statement and patient consent

The TRANSFORM I study was conducted in accordance with the Declaration of Helsinki and was approved by the institutional review board or ethics committee at each participating center. Written informed consent was obtained from all participants before enrollment.

Supplementary material

To access the supplementary material accompanying this article, visit the online version of the *Journal of the Society for Cardiovascular Angiography & Interventions* at 10.1016/j.jscai.2026.105674.

References

1. Fezzi S, Serruys PW, Cortese B, et al. Indications for use of drug-coated balloons in coronary intervention: Academic Research Consortium position statement. *J Am Coll Cardiol*. 2025;86(15):1170–1202. https://doi.org/10.1016/j.jacc.2025.07.049
2. Fezzi S, Scheller B, Cortese B, et al. Definitions and standardized endpoints for the use of drug-coated balloon in coronary artery disease: consensus document of the Drug Coated Balloon Academic Research Consortium. *Eur Heart J*. 2025;46(26):2498–2519. https://doi.org/10.1093/eurheartj/ehaf029
3. Fezzi S, Giacoppo D, Fahrni G, et al. Individual patient data meta-analysis of paclitaxel-coated balloons vs. drug-eluting stents for small-vessel coronary artery disease: the ANDROMEDA study. *Eur Heart J*. 2025;46(17):1586–1599. https://doi.org/10.1093/eurheartj/ehaf002
4. Rissanen TT, Uskela S, Eränen J, et al. Drug-coated balloon for treatment of de-novo coronary artery lesions in patients with high bleeding risk (DEBUT): a single-blind, randomised, non-inferiority trial. *Lancet*. 2019;394(10194):230–239. https://doi.org/10.1016/S0140-6736(19)31126-2
5. Jeger RV, Farah A, Ohlow MA, et al. Drug-coated balloons for small coronary artery disease (BASKET-SMALL 2): an open-label randomised non-inferiority trial. *Lancet*. 2018;392(10150):849–856. https://doi.org/10.1016/s0140-6736(18)31719-7
6. Jeger RV, Farah A, Ohlow MA, et al. Long-term efficacy and safety of drug-coated balloons versus drug-eluting stents for small coronary artery disease (BASKET-SMALL 2): 3-year follow-up of a randomised, non-inferiority trial. *Lancet*. 2020;396(10261):1504–1510. https://doi.org/10.1016/s0140-6736(20)32173-5
7. Serruys PW, Tobe A, Ninomiya K, et al. Is the axiom of balloon angioplasty, "the more you gain the more you lose," still true in the era of DCB with paclitaxel? *Cardiovasc Revasc Med*. 2024;69:70–78. https://doi.org/10.1016/j.carrev.2024.04.001
8. Tobe A, Serruys P, Miyashita K, et al. Serial quantitative optical coherence tomography for luminal volume changes following either paclitaxel or sirolimus coated balloon in de novo small coronary artery lesions. *Cardiovasc Revasc Med*. 2025;81:62–67. https://doi.org/10.1016/j.carrev.2025.03.025
9. Yamamoto M, Hara H, Kubota S, Hiroi Y. Predictors of late lumen enlargement after drug-coated balloon angioplasty for de novo coronary lesions. *EuroIntervention*. 2024;20(9):602–612. https://doi.org/10.4244/EIJ-D-23-00849
10. Yamamoto T, Kawamori H, Toba T, et al. Clinical impact of optical coherence tomography findings after drug-coated balloon treatment for patients with acute coronary syndromes. *Int J Cardiol*. 2023;387:131149. https://doi.org/10.1016/j.ijcard.2023.131149
11. Lee T, Ashikaga T, Nozato T, et al. Predictors of target lesion failure after percutaneous coronary intervention with a drug-coated balloon for de novo lesions. *EuroIntervention*. 2024;20(13):e818–e825. https://doi.org/10.4244/EIJ-D-23-01006
12. Kume T, Akasaka T, Kawamoto T, et al. Assessment of coronary arterial thrombus by optical coherence tomography. *Am J Cardiol*. 2006;97(12):1713–1717. https://doi.org/10.1016/j.amjcard.2006.01.031
13. Ali ZA, Karimi Galougahi K, Mintz GS, Maehara A, Shlofmitz RA, Mattesini A. Intracoronary optical coherence tomography: state of the art and future directions. *EuroIntervention*. 2021;17(2):e105–e123. https://doi.org/10.4244/EIJ-D-21-00089
14. Jawien A, Bowen-Pope DF, Lindner V, Schwartz SM, Clowes AW. Platelet-derived growth factor promotes smooth muscle migration and intimal thickening in a rat model of balloon angioplasty. *J Clin Invest*. 1992;89(2):507–511. https://doi.org/10.1172/jci115613
15. Giese NA, Marijianowski MM, McCook O, et al. The role of alpha and beta platelet-derived growth factor receptor in the vascular response to injury in nonhuman primates. *Arterioscler Thromb Vasc Biol*. 1999;19(4):900–909. https://doi.org/10.1161/01.atv.19.4.900
16. Huang B, Dreyer T, Heidt M, et al. Insulin and local growth factor PDGF induce intimal hyperplasia in bypass graft culture models of saphenous vein and internal mammary artery. *Eur J Cardiothorac Surg*. 2002;21(6):1002–1008. https://doi.org/10.1016/s1010-7940(02)00111-2
17. Hsu MJ, Hsiao S-H, Lien JC, Huang TF, Huang YH, Huang SW. Nstpbp5185, a novel benzimidazole derivative, suppresses PDGF signaling and reduces neointimal hyperplasia following vascular injury. *Eur J Pharmacol*. 2026;1021:178824. https://doi.org/10.1016/j.ejphar.2026.178824
18. Ninomiya K, Serruys PW, Colombo A, et al. A prospective randomized trial comparing sirolimus-coated balloon with paclitaxel-coated balloon in de novo small vessels. *JACC Cardiovasc Interv*. 2023;16(23):2884–2896. https://doi.org/10.1016/j.jcin.2023.09.026
19. Kaivosoja TP, Liu S, Dijkstra J, Huhtala H, Sheth T, Kajander OA. Comparison of visual assessment and computer image analysis of intracoronary thrombus type by optical coherence tomography. *PLoS One*. 2018;13(12):e0209110. https://doi.org/10.1371/journal.pone.0209110
20. Tu S, Ding D, Chang Y, Li C, Wijns W, Xu B. Diagnostic accuracy of quantitative flow ratio for assessment of coronary stenosis significance from a single angiographic view: a novel method based on bifurcation fractal law. *Catheter Cardiovasc Interv*. 2021;97(Suppl 2):1040–1047. https://doi.org/10.1002/ccd.29592
21. Tobe A, Miyashita K, Revaiah PC, et al. Precision and accuracy of dimensional assessment of luminal contours by commercially available quantitative angiography software as a prerequisite to angiography based FFR and other derived parametrics. *Catheter Cardiovasc Interv*. 2025;106(2):1162–1172. https://doi.org/10.1002/ccd.31670
22. Garin D, Arroyo D, Iglesias JF, et al. Coronary angiography-derived Murray law-based quantitative flow ratio (μQFR) after de novo drug-coated balloon angioplasty. *Catheter Cardiovasc Interv*. 2025;106(5):2935–2944. https://doi.org/10.1002/ccd.70150
23. Sato Y, Hatakeyama K, Yamashita A, Marutsuka K, Sumiyoshi A, Asada Y. Proportion of fibrin and platelets differs in thrombi on ruptured and eroded coronary atherosclerotic plaques in humans. *Heart*. 2005;91(4):526–530. https://doi.org/10.1136/hrt.2004.034058
24. Baaten CCFMJ, Nagy M, Bergmeier W, Spronk HMH, van der Meijden PEJ. Platelet biology and function: plaque erosion vs. rupture. *Eur Heart J*. 2024;45(1):18–31. https://doi.org/10.1093/eurheartj/ehad720
25. Kay IP, Ligthart JMR, Virmani R, et al. The black hole: echolucent tissue observed following intracoronary radiation. *Int J Cardiovasc Intervent*. 2003;5(3):137–142. https://doi.org/10.1080/14628840310007673
26. van der Meijden PEJ, Heemskerk JWM. Platelet biology and functions: new concepts and clinical perspectives. *Nat Rev Cardiol*. 2019;16(3):166–179. https://doi.org/10.1038/s41569-018-0110-0
27. Prati F, Guagliumi G, Mintz GS, et al. Expert review document part 2: methodology, terminology and clinical applications of optical coherence tomography for the assessment of interventional procedures. *Eur Heart J*. 2012;33(20):2513–2520. https://doi.org/10.1093/eurheartj/ehs095
28. Ding Y, Abbasi M, Eltanahy AM, et al. Assessment of blood clot composition by spectral optical coherence tomography: an in vitro study. *NeuroIntervention*. 2021;16(1):29–33. https://doi.org/10.5469/neuroint.2020.00297